Ref.TH.2310-CERN

ANALYSIS OF THE Λp ENHANCEMENT AT 2.129 GeV IN THE REACTION $K^-d \to \pi^- \Lambda p$

H.G. Dosch *) and V. Hepp **)

CERN -- Geneva

A B S T R A C T

Analyzing the cross-section of the reaction $K^-d \to \pi^- \Lambda p$ in the region of the invariant Λp mass of 2.129 GeV we show that this enhancement is the combined effect of a cusp due to the deuteron and a sharp maximum in the scattering matrix element for the reaction $\Sigma N \to \Lambda N$ at $m_{\Lambda p} \approx 2.125$-$2.127$ GeV. This indicates the existence of a Λp resonance at this energy and a ΣN bound state decaying into Λp.

---

*) On leave of absence from Institut für Theoretische Physik, Universität Heidelberg, Germany.

**) Present address : Institut für Hochenergie-Physik, Universität Heidelberg, Germany.

Ref.TH.2310-CERN
20 April 1977

1. - INTRODUCTION

In this paper we investigate the enhancement of the cross-section for the reaction $K^- d \to \pi^- \Lambda p$ near the invariant Λp mass of 2.129 GeV [1),2)]. It is somewhat discomforting that this enhancement is just at the $\Sigma^+ n$ threshold and hence could be due to a purely kinematical effect : since the reaction $\Sigma N \to \Lambda N$ is exothermic, the cross-section for this reaction near threshold shows the $1/v$ (flux factor) enhancement, even if the T matrix element for this reaction is perfectly smooth. In the deuteron reaction the mass of the (virtual) ΣN system can also be below threshold and hence the reaction for a smooth T matrix element of $\Sigma \Lambda \to \Lambda N$ shows a cusp just at threshold. We try in this paper to disentangle the deuteron dynamics from the dynamics of the hyperon-nucleon scattering. We will show that, though the cusp due to deuteron dynamics is similar to the observed effects, the nevertheless characteristic differences necessitate a sharp maximum in the $^3S_1$ $\Sigma N \to \Lambda P$ scattering matrix element at a Λp effective mass of 2.125 to 2.127 GeV.

2. - THEORETICAL MODEL

Contributions to the reaction $K^- d \to \pi^- \Lambda p$ are presented graphically in a kind of skeleton diagrams in Fig. 1. There and in the following, d, M ; p, m_p ; n, m_n ; Λ, m_Λ ; Σ, m_Σ ; K, m_K ; π, m_π denote the four-momenta and masses of the deuteron, proton, neutron, Λ hyperon, Σ hyperon, K meson and π meson, resp., N, m_N denotes nucleon momentum or mass. Furthermore, we use $s = (K + d)^2$, $w = (K - \pi)^2$, $t = (d - p)^2$; Θ^* angle between K and π in the Kd rest frame. The amplitude corresponding to diagram 1a gives the dominant contribution for values of t near m_n^2. Contribution 1c gives the enhancement at ΣN threshold mentioned in Section 1, even if the T matrix element at the reaction $\Sigma N' \to \Lambda N$ is constant ; diagram 1b should be of some importance if there is an enhancement in the T matrix element for the reaction $\Lambda N' \to \Lambda N$ (which problem we are just investigating) ; 1e and 1f should give a small, and in the variable v, very smooth background ; they are omitted in the following considerations.

The amplitude corresponding to 1a is :

$$T^{(a)} = \frac{-1}{(2\pi)^{15/2}} \int \bar{u}_\alpha(\Lambda)\, T_{\alpha\beta}(K N'; \pi\Lambda) \cdot$$

$$\frac{(\gamma N' + m_n^2)_{\beta\gamma}}{t - m_n^2 + i\varepsilon}\, \Gamma_{\gamma\delta}(t)\, \bar{u}_\delta(p) \cdot$$

$$\delta^4(N' - d - p)\, \delta^4(N' + K - \pi - \Lambda)\, d^4 N' \qquad (2.1)$$

u are spinors, $\Gamma(t)$ is the relativistic d-N-N vertex with one nucleon on-mass shell, $\bar{u}(\Lambda)T(K,N';\pi\Lambda)u(N).(1/(2\pi)^6)$ is the on-mass shell T matrix element for $KN - \pi\Lambda$ scattering.

The amplitudes 1b, 1c have the same structure :

$$T^{(b,c)} = \frac{1}{(2\pi)^{15/2}} \frac{1}{(2\pi)^4} \int \bar{u}_\alpha(\Lambda)\, \bar{u}_\beta(p)\, T_{\alpha\beta;\delta\varepsilon}(Y', N'; \Lambda p)$$

$$\frac{(\gamma Y' + m_{Y'})_{\delta\eta}}{Y'^2 - m_{Y'}^2 + i\varepsilon}\; \frac{(\gamma N' + m_{N'})_{\varepsilon\zeta}}{N'^2 - m_{N'}^2 + i\varepsilon}\; T_{\eta\vartheta}(K N; \pi Y')$$

$$\frac{(\gamma N + m_N)_{\vartheta\varphi}}{N^2 - m_N^2 + i\varepsilon}\; \Gamma_{\varphi\zeta}(N'^2, N^2) \cdot \delta^4(Y' + N' - \Lambda - p)$$

$$\delta^4(Y' + \pi - N - K)\, \delta^4(d - N - N') \qquad (2.2)$$

$$d^4 Y'\, d^4 N'\, d^4 N \quad .$$

$\bar{u}_\alpha(\Lambda)\, \bar{u}_\beta(p)\, T_{\alpha\beta;\delta\varepsilon}(Y' N'; \Lambda p)\, u_\delta(Y')\, u_\varepsilon(N')(1/2\pi)^6$ is the T matrix element for the reaction $Y + N' \to \Lambda p$; $\Gamma(N'^2, N^2)$ is the deuteron form factor with the two nucleons off-mass shell, Y stands for Λ and Σ.

Before we make approximations in order to bring these equations into a form easy to evaluate, we discuss some general properties of $T^{b,c}$.

If v reaches the ΣN threshold from below, diagram 1c becomes internally unstable and the amplitude develops an absorptive part in this variable. This onset of an absorption part gives rise to a sharp cusp in the dispersive part of the amplitude. The position of this cusp is uniquely determined by the physical masses in the denominators of the propagators to be at $v = (m_N + m_\Sigma)^2$; the contribution of 1b does not show such a structure. Also the w dependence of $T^{b,c}$ depends considerably on the values of v. Near the region of internal instability [i.e., $v = (m_\Lambda + m_N)^2$ for 1b, $v = (m_N + m_\Sigma)^2$ for 1c] the anomalous threshold in w is, on the physical sheet, very near the physical region and hence gives rise to a very marked fall-off in w, hence T^c decreases rapidly in w near $v = (m + m_\Sigma)^2$. Both features can be understood intuitively : the cusp is just a reflection of the $1/v$ law and the fast fall-off with w is just the rapidly falling form factor of a loosely bound (or nearly bound) system. We will discuss these features quantitatively later.

We now make some approximations in order to evaluate (2.1) and (2.2).

1) The numerators of the Fermion propagators are replaced by their "mass shell values" :

$$(\gamma N + m)_{\alpha\beta} \longrightarrow 2m \; u_\alpha(N)\, \bar{u}_\beta(N)$$

2) The meson-baryon scattering amplitude is replaced by its mass shell value ; these approximations are motivated by the loose structure of the deuteron, which lets the main contributions come from values of the internal momenta near mass shell.

3) We replace

$$\bar{u}(N')\,\Gamma(N'^2, N^2)\, u(N) \longrightarrow \chi' \vec{\sigma}\vec{\xi}\; i\sigma_2 \chi \; F(N^2, N'^2)$$

where $\vec{\xi}$ is the polarization vector of the deuteron ; by that we neglect the D wave contribution and some relativistic effects.

4) For Y-N scattering amplitudes we only take into account the S wave contributions.

5) In T^b and T^c we take $T(KN,\pi Y)$ out of the integral at the value $\vec{N} = \vec{d}/2$. This is the most important simplification. It is the better justified, the less $T(KN,\pi Y)$ varies with the scattering angle. It is better justified for $s = 7.13\ \mathrm{GeV}^2$ than for $s = 8.5\ \mathrm{GeV}^2$, where the dominant contribution $\mathrm{Re}\ f^{\Sigma^+}$ depends strongly on the scattering angle.

With these approximations, we are led to

$$T^a = \frac{-2m}{(2\pi)^{15/2}} \chi^\Lambda \left[f(\tilde{s}, \cos\vartheta) + i g(\tilde{s}, \cos\vartheta)\, \vec{\sigma}\cdot\vec{n} \right] \sigma\xi \; i\sigma_2 \chi^p \; (2\pi)^5 \frac{2\sqrt{\tilde{s}}}{\sqrt{m_n m_\Lambda}} F(t) \frac{1}{t - m_n^2} \qquad (2.3)$$

$$\begin{aligned} T^{b,c} = {} & \mathrm{sign}\,Y \frac{1}{(2\pi)^{15/2}} (2m_N)^2 \cdot 2m_Y\, \mathcal{F}(\omega\cdot v; Y) \\ & \chi^\Lambda \{ 4 t_t^Y(v)\, f^Y(\tilde{s}', \cos\vartheta') \cdot \sigma\xi \\ & - 4 t_t^Y(v) [\vec{n}\times\vec{\xi}]\, g^Y(\tilde{s}', \cos\vartheta') + \\ & 4i\, t_s(v)\, \vec{n}\cdot\vec{\xi}\, g^Y(\tilde{s}', \cos\vartheta') \} \cdot i\sigma_2 \chi^p \; . \end{aligned} \qquad (2.4)$$

$F(t)$ is the deuteron form factor, f^Y and g^Y are the spin-non-flip and spin-flip amplitudes for the reaction $KN \to \pi Y$:

$$\chi^Y (f + i\vec{\sigma}\vec{n}\, g) \chi^N = \bar{u}(Y)\, T(KN; \pi Y)\, u(N) \; .$$

In T^a angle and energy are determined by the kinematical configuration : $\vec{K}$, $\vec{\pi}$, $\vec{Y} = \vec{\Lambda}$, in $T^{b,c}$ by K, $\vec{\pi}$, $\vec{N} = \vec{d}/2$. t_s^Y and t_t^Y are the singlet and triplet hyperon-nucleon scattering amplitudes.

$$\begin{aligned} & \bar{u}(\Lambda)\, \bar{u}(p)\, T(YN; \Lambda p)\, u(Y)\, u(N) = \\ & \frac{(2\pi)^5}{\sqrt{v}} \chi^\Lambda_\alpha \chi^p_\beta \{ (t_s + 3t_t)\, \delta_{\alpha\delta}\, \delta_{\beta\varepsilon} \\ & + (t_t - t_s)\, \vec{\sigma}_{\alpha\delta} \cdot \vec{\sigma}_{\beta\varepsilon} \} \chi^Y_\delta \chi^N_\varepsilon \; . \end{aligned}$$

$$\mathcal{F}(v, w; Y) =$$

$$\int d^4k \frac{F\left((p+\Lambda-k)^2, (k+d-p-\Lambda)^2\right)}{(k^2-m_Y^2+i\varepsilon)\left((\Lambda+p-k)^2-m_N^2+i\varepsilon\right)\left((k+d-p-\Lambda)^2-m_N^2+i\varepsilon\right)}$$

(2.5)

sign $Y = +1$ for Λ and Σ^0, -1 for Σ^+.

Since we are mainly interested in the behaviour of $\mathcal{F}(v,w,Y)$ near $v = (m_N + m_\Sigma)^2$ we evaluate it by dispersion techniques [3] :

$$\mathrm{Re}\,\mathcal{F}(v, w; Y) = \frac{P}{2\pi i} \int_{(m+m_Y)^2}^{\infty} \frac{\mathrm{Disc}\,\mathcal{F}(v', w; Y)}{v' - v}\, dv' \qquad (2.6)$$

$$\mathrm{Disc}\,\mathcal{F}(v, w; Y) = (2\pi i)^2 \cdot$$
$$\int d^4k \frac{F\left((p+\Lambda-k)^2, (k+d-p-\Lambda)^2\right)}{(k+d-p-\Lambda)^2-m_N^2+i\varepsilon}\, \delta(k^2-m_Y^2)\, \delta\left((p+\Lambda-k)^2-m_N^2\right) \qquad (2.7)$$

From (2.6) follows that the form of $\mathcal{F}(v,w,Y)$ near $v = (m + m_\Sigma)^2$ is uniquely determined by $F(m_N^2, (k + d - p - \Lambda)^2) = F((k + d - p - \Lambda)^2)$, the deuteron form factor with one nucleon mass shell.

This deuteron form factor is here taken as a relativistic generalization of the Hultèn wave function :

$$F(t) = \frac{8\sqrt{2\pi}}{\sqrt{M}} \sqrt{(\alpha+\beta)^3\, \alpha\beta}\; \frac{1}{t - m_N^2 - 2\beta^2 + 2\alpha^2}$$

$$\alpha = \sqrt{2 m_N \cdot E_B} = 0.045 \text{ GeV} \qquad \beta = .2548 \text{ GeV}$$

The functions $\mathcal{F}(v,w,Y)$ show the features discussed above. Their square module for several values of v and w is given in Fig. 2. The fast decrease of $\mathcal{F}(v,w,\Sigma)$ with w (or correspondingly $\cos\Theta^*$) can be seen from Fig. 2. The increase of $|\mathcal{F}(v,w(\cos\Theta^*),\Lambda|^2$ with Θ^* near $\cos\Theta^*=1$ and $v \approx (m+m_{\Sigma}^2)$ can also be understood intuitively : the crossing Λ' in Fig. 1c has to get some momentum in order to form with N' the invariant mass $v \approx (m_N + m_{\Sigma})^2$ which is c. 80 MeV above $(m_N + m_{\Lambda})^2$.

3. - COMPARISON WITH EXPERIMENTAL DATA

We analyze in the theoretical framework discussed in Section 2 the experimental data of Ref. 1) $(s = 9.5\ GeV^2)$ and Ref. 2) $(s = 7.13\ GeV^2)$. In order to test the hypothesis that the enhancement is determined purely by deuteron dynamics and not by a pronounced structure in the Y-N amplitudes, we evaluate the contribution of graph 1c. Since we analyze only data with $\cos\Theta^* \geq 0.8$, we neglect the spin-flip amplitude g in Eq. (2.4) and hence t_s^Y does not contribute. For f we insert values determined from the parameters of the phase shift analysis of Ref. 4). In this test we put $t^{\Sigma^+} = \sqrt{2}t^{\Sigma^o} = \text{const.}$ and obtain the results of Fig. 3.

In both experiments we see indeed the cusp mentioned above, but in both experiments the observed experimental peak is below the cusp. Furthermore, the cusp falls off much more slowly at v values above its peak value than the experimental curves ; the latter ones look indeed rather similar in both experiments. The difference in the theoretical curves is mostly due to the different w region corresponding to the range $1 \geq \cos\Theta^* \geq 0.9$ at $s = 7.13$ and $9.5\ GeV^2$, resp. The different $KN \to Y\pi$ scattering amplitudes play also an important rôle. For the energy of Ref. 2) $(s = 7.13\ GeV^2)$ practically only the Σ^o contributes, whereas at $s = 9.5$ [Ref. 1)] the Σ^+ contribution is dominant.

In order to demonstrate that the hypothesis of slowly varying hyperon-nucleon scattering matrix elements is incompatible with the data, we subtract the "background" contribution 1a *) from the experimental data. We then form the ratio of this corrected cross-section to the theoretical one with $t_t^{\Sigma^+} = \sqrt{2} t_t^{\Sigma^0} = (\sqrt{2}/\sqrt{3})$ GeV^{-1}. The result can be seen in Fig. 4. This figure shows clearly that t_t^{Σ} must have a rather pronounced maximum at $\sqrt{v'} \sim 2.127$ GeV. There is a characteristic difference for this ratio R for both experiments : the data at higher energies yield a value for R which is lower and whose maximum is rather at $\sqrt{v} = 2.125$ GeV than at 2.127 GeV. Since the theoretical analysis of the data at $s = 9.5$ GeV^2 suffers from the fact that the most important contribution to the $KN \to \Sigma\pi$ amplitude, namely Re $f^{\Sigma+}$, depends very strongly on the scattering angle, this difference in R can be partly due to it. On the other hand, the Σ^0 mainly contributes at $s = 7.13$ GeV^2, and the Σ^+ mainly contributes at $s = 9.5$ GeV^2 ; both these contributions may be rather different. Though both are pure isospin $I = \frac{1}{2}$ (due to the final state Λp) the mass splitting is of the same order as the "binding energy" [i.e., the difference between the peak in t^{Σ} and $(m + m_{\Sigma})$], and hence isospin breaking may be important.

In order to get an idea on the values of the scattering matrix elements, we make an ansatz for those determined by the K matrix formalism [5]. As mentioned above, isospin breaking is important near threshold and one ought to make a six-channel analysis :

$$\Lambda p \to \Lambda p\,, \quad \Sigma^0 p \to \Sigma^0 p\,, \quad \Sigma^+ n \to \Sigma^+ n\,, \quad \Sigma^+ n \to \Sigma^0 p\,,$$

$$\Sigma^0 p \to \Lambda p\,, \quad \Sigma^+ n \to \Lambda p$$

necessitating, even in zero range approximation, six parameters. With present statistics not allowing such a length parameter fit, we analyze the experiments of Ref. 1) with the ansatz :

$$t^{\Sigma^+} = \sqrt{2}\, t^{\Sigma^0} = \sqrt{(2/3)}\, \cdot t^{(1/2)}$$

---

*) A comparison of the predicted direct Λ production with the experimental data of Ref. 2) shows a satisfactory agreement of the cross-sections. The rapid fall-off of $d\sigma/dv$ with increasing v is well reproduced.

For $t_t^{(\frac{1}{2})}$ and t_t^{Λ} we put

$$t_t^{\Lambda} = -\{\varphi_\Lambda(1+iq_\Sigma\varphi_\Sigma) - i\,q_\Sigma\,\varphi_{\Sigma\Lambda}^2\}/D$$

$$t^{(1/2)} = -\varphi_{\Sigma\Lambda}/D$$

$$D = (1+i\,q_\Lambda\varphi_\Lambda)(1+iq_\Sigma\varphi_\Sigma) + q_\Lambda q_\Sigma\varphi_{\Sigma\Lambda}^2$$

q_Σ and q_Λ are the hyperon momenta in the Y-N rest frame. Since at $s = 7.13$ mainly the Σ^o contributes, we take for q_Σ the Σ^o momentum *).

The φ_Y are, in the physical region, real functions which, apart from possible poles, have only dynamical singularities. The data of Ref. 2) near $\sqrt{v} = 2.127$ GeV are well described by the set $\varphi_\Lambda = 0$, $\varphi_\Sigma = 20$ GeV^{-1}, $\varphi_{\Sigma\Lambda} = -7$ GeV^{-1} **). A better fit can be obtained by making $\varphi_{\Sigma\Lambda}$ v dependent. In Figs. 5 and 6 we give the results for the choice

$$\varphi_\Lambda = 0\ ,\quad \varphi_\Sigma = 20\ \text{GeV}^{-1}$$

$$\varphi_{\Sigma\Lambda} = -7.5\ [\text{GeV}]^{-1} - 150\,(v - (m_N + m_\Sigma)^2)$$

v in GeV^2.

We see that not only the v dependence but also the w dependence is quite well reproduced. Due to the shift of the maximum seen in Fig. 4 we expect a smaller value of φ_Σ from the data of Ref. 1). Indeed here we get a best (but not very good) fit with $\varphi_\Sigma = 10$, $\varphi_{\Sigma\Lambda} = -7$ GeV. A more detailed analysis at the scattering parameters, also including the direct scattering cross-sections, is in preparation.

---

*) The sign convention here corresponds in the single channel formalism $\varphi = -(1/q)\ \text{tg}\ \delta$.

**) The data favour small values of φ_Λ, but the dependence is not very crucial. Note that we are c. 80 MeV above threshold, so even a small value of φ_Λ does by no means imply a small Λp scattering length.

4. - DISCUSSION AND CONCLUSION

The present analysis of the data of Ref. 1) and Ref. 2) shows that the enhancement of the (Λp) invariant mass at 2.129 GeV cannot be explained by a cusp due to deuteron dynamics for two reasons :

1) the peak of the cusp is, for the data of both Ref. 1) and Ref. 2), 4 MeV above the observed one ;
2) the form of the observed enhancement is distinctly different from the "deuteron-dynamical" cusp. Since the form and especially the position of the cusp is independent of the detailed assumptions made, we think these arguments to be very decisive.

The $\cos\theta^*$ dependence of the cross-section near $\sqrt{v} = 2.127$ GeV observed in Ref. 2) shows that the effect must be mainly due to $\Sigma N \rightarrow \Lambda p$ (Fig. 1c) and not to $\Lambda p - \Lambda p$ final state interaction (Fig. 1b). The fact that it occurs in forward direction implies the enhancement in the spin triplet channel. The cusp due to the internal instability of 1c has, however, an important effect on the apparent position of the enhancement. As can be seen from Fig. 4, the maximum of t_t^{Σ} is reached at $\sqrt{v} = 2.125$ or 2.127 GeV rather than at the observed peak at 2.129 GeV^2. This maximum corresponds to a (ΣN) $I = \frac{1}{2}$, ${}^tS_1$ bound state, decaying into Λp. Of course, it induces also a Λp resonance in this channel.

There seems also to be a rather important difference between the scattering matrix elements of the reactions $\Sigma^+ n \rightarrow \Lambda p$ and $\Sigma^o p \rightarrow \Lambda p$. We are, however, well aware that this statement depends much more on the detailed assumptions made in our analysis.

Our treatment differs from the one of Satoh, Iwamura and Takahashi [6)] in two respects : we first try to separate clearly the deuteron effects from those of the hyperon-nucleon scattering, and secondly calculate contribution 1c also above ΣN threshold. We agree with their conclusion about the fact that the properties of the triangle graph 1c cannot explain alone the observed enhancement, but we disagree about the position of the maximum of $|t_t^{\Sigma}|^2$.

The difference between our treatment and that of Alexander et al. [7)] is clear. By taking only rescattering of on-mass shell Σ hyperon into account, they only take the absorptive part of contribution 1c, whereas for the form of the cusp the dispersive part is very important (see Fig. 2c).

Deuteron effects therefore give, in their treatment, a peak which is higher and broader than the one obtained by us (Fig. 3). There are numerous predictions for a $\Sigma\Lambda$ bound state / Λp resonance [8),9),10)]. A better determination of the scattering parameter which would necessitate much higher statistics of the experiments would be especially interesting in order to distinguish between a conventional bound state [Ref. 9)] and the six-quark in a bag state of Ref. 10).

ACKNOWLEDGEMENTS

It is a pleasure to thank G. Ekspong, T. Ericson, L. Montanet, F. Myhrer and C. Roos for useful discussions.

REFERENCES

1) D. Eastwood, J.R. Fry, F.R. Heathcote, G.S. Islam, D.J. Candlin, G. Copley, G.R. Evans, J.R. Campbell, W.T. Morton, P.J. Negus, M.J. Counihan, D.P. Goyal, D.B. Miller and B. Schwarzschild - Phys.Rev. D3, 2603 (1971).

2) O. Braun, H.J. Grimm, V. Hepp, H. Stroebele, C. Thoel, T.J. Thouw, F. Gandini, C. Kiesling, D.E. Plane and W. Wittek - Preprint to appear in Nuclear Phys. ;

V. Hepp - Topical Conference on Baryon Resonances, Oxford (1976). See also the literature quoted there for earlier experiments.

3) R.E. Cutkosky - J.Math.Phys. 1, 429 (1960).

4) G.P. Gopal, R.T. Ross, A.J. Van Horn, A.C. McPherson, E.F. Clayton, T.C. Bacon and I. Butterworth - Nuclear Phys. B119, 362 (1977).

5) See, for instance :

R.H. Dalitz and S.F. Tuan - Ann.Phys. 3, 307 (1960), and Ref. 9).

6) E. Satoh, Y. Iwamura and Y. Takahashi - Phys.Rev.Letters 35, 1128 (1975).

7) G. Alexander, B.H. Hall, N. Jew, C. Kalmus and A. Kernan - Phys.Rev. Letters 22, 483 (1969).

8) R.J. Oakes - Phys.Rev. 131, 2239 (1963).

9) J.J. de Swart, M.M. Nagels, T.A. Rijken and P.A. Verhoeven - Springer Tracts of Physics 60, 138 (1971) ;

M.M. Nagels, T.A. Rijken and J.J. de Swart - Ann.Phys. 79, 338 (1973).

10) R.L. Jaffe - Phys.Rev.Letters 38, 195 (1977).

FIGURE CAPTIONS

Figure 1 Graphical description of contributions to the reaction $K^- d \to \pi^- \Lambda p$.

a) direct production (simple impulse approximation) ;

b),c) hyperon-nucleon final state interaction ;

d),e) rescattering corrections not taken into account in the present analysis.

Figure 2 a),b)

$$\frac{1}{0.002}\int_{\sqrt{v}-0.001}^{\sqrt{v}+0.001} d\sqrt{v'}\,|\mathcal{F}(v', w(s,\cos\vartheta^*); Y|^2 \qquad \text{vs. } \sqrt{v}$$

with × $(w(s=7.13,\ \cos\theta^*=1)$

○ $w(s=7.13,\ \cos\theta^*=0.9)$

(a) $Y=\Sigma^0$; (b) $Y=\Lambda$

The binning in intervals of 2 MeV is done in analogy with the experiments, Refs. 1), 2).

c) Re $\mathcal{F}(v,w(7.13,1),\Sigma^0)$ and Im $\mathcal{F}(v,w(7.13),\Sigma^0)$

——— real (dispersive) part

------ imaginary (absorptive) part.

Figure 3

$$\sigma = \int_1^{0.9} d\cos\vartheta \int_{\sqrt{v_i}-0.001}^{\sqrt{v_i}+0.001} d\sqrt{v}\ \sigma(v, \cos\vartheta)$$

at two different energies (averaged over deuteron and summed over fermion on spins).

○ Experimental cross-section (GeV^{-2}) ;

× contribution of 1c (Σ^0 and Σ^+, with $t^{\Sigma^+} = \sqrt{2}\, t^{\Sigma^0} = \text{const}$) arbitrary units.

(a) $s = 7.13\ GeV^2$; (b) $s = 9.5\ GeV^2$.

Figure 4 Ratio of "background" corrected experimental cross-section to theoretical best cross-section with constant t^{Σ}.
$R = (\sigma^{exp} - \sigma^{a})/\sigma_{o}$ where σ^{a} is the contribution of graph 1a, σ_{o} is the contribution of 1c with $t^{\Sigma^+} = \sqrt{2} . t^{\Sigma^o} = 1/\sqrt{3}$ GeV^{-1}.
σ defined as in Fig. 3.

- Experimental data at $s = 7.13$ GeV^2, Ref. 2) ;
- Experimental data at $s = 9.5$ GeV^2, Ref. 1).

Figure 5 $\sqrt{v}$ dependence.

$$\sigma = \int_{.9}^{1} d\cos\vartheta \int_{\sqrt{v}-0.001}^{\sqrt{v}+0.001} d\sqrt{v'}\ \sigma(v', \cos\vartheta)$$

- O Experimental data of Ref. 2) ($s = 7.13$) ;
- X Theory : contribution 1a, 1b, 1c,

$$\varphi_{\Lambda} = 0\ ,\ \varphi_{\Sigma} = 20,\ \ \varphi_{\Sigma\Lambda} = -7.5 - 150 \cdot [v - (m_N + m_{\Sigma})^2]$$

all values in GeV^{-1} and GeV^2, resp.

Figure 6 Angular distribution.

$$\sigma = \int_{\cos\vartheta - 0.025}^{\cos\vartheta + 0.025} d\cos\vartheta' \int_{\sqrt{v}-0.002}^{\sqrt{v}+0.002} d\sqrt{v'}\ \sigma(v', \cos\vartheta')$$

- O Experimental data
- X Theory as in Fig. 5.

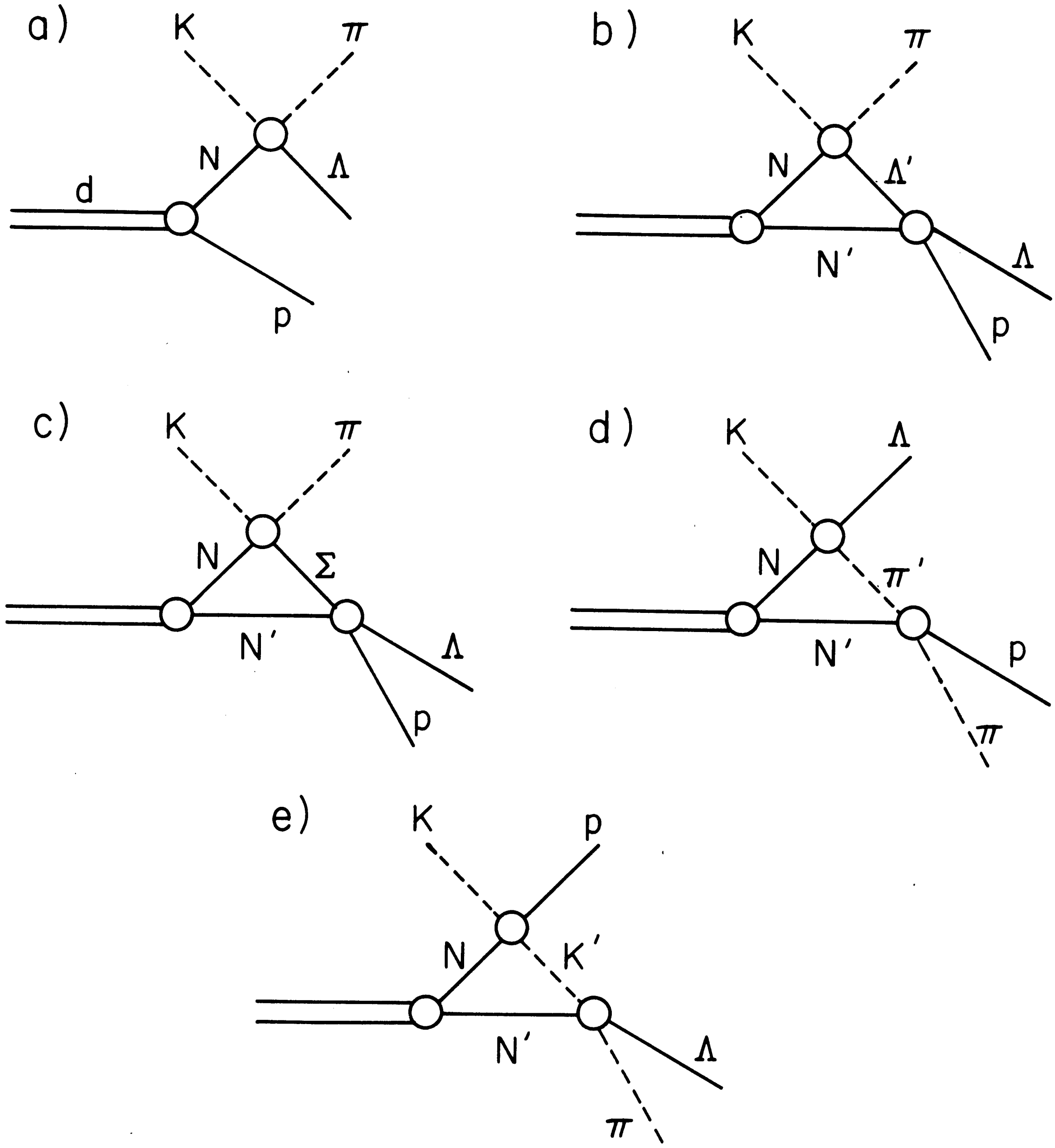

FIG. 1

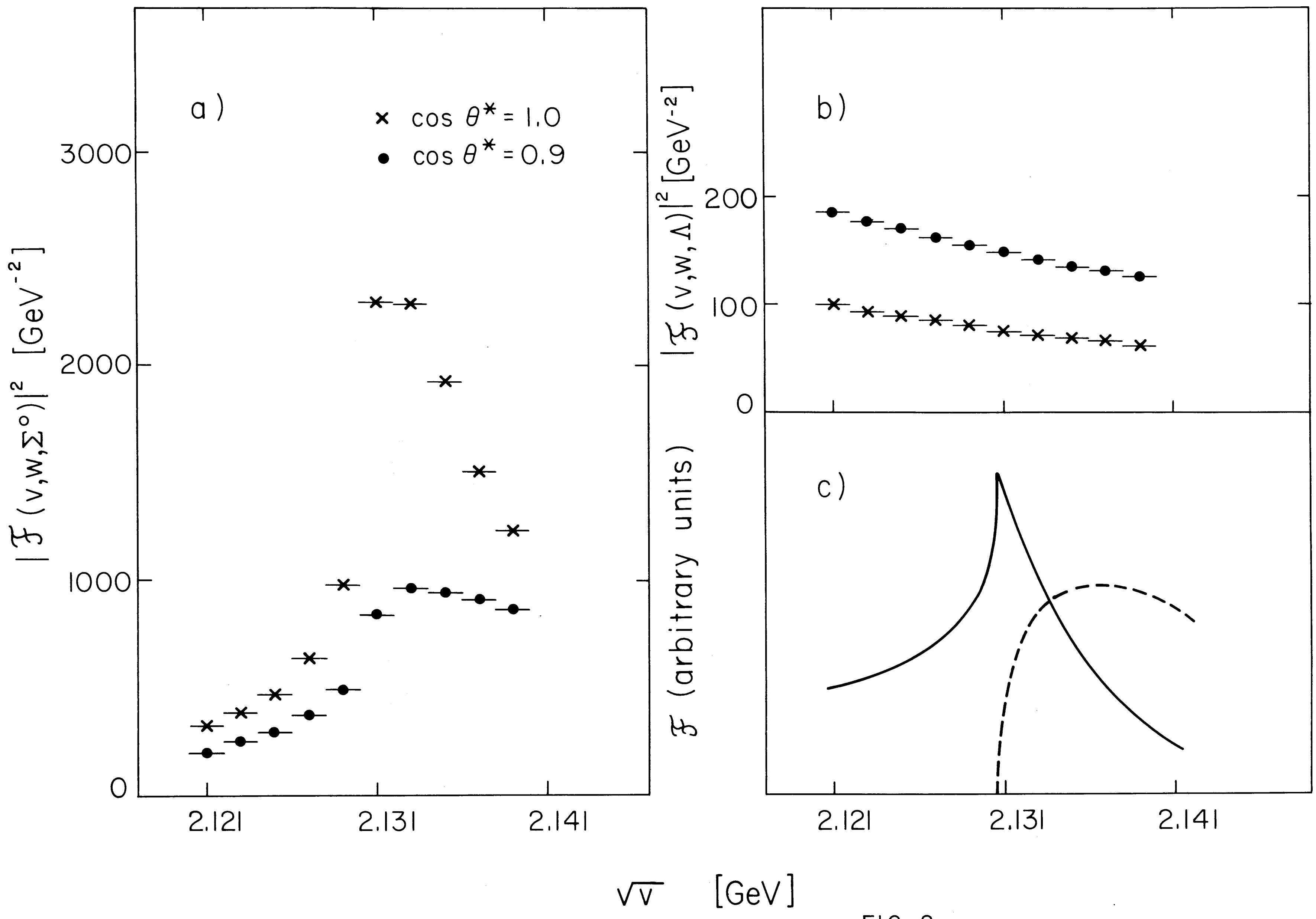
a)
× cos θ* = 1.0
● cos θ* = 0.9
|𝓕 (v,w,Σ°)|² [GeV⁻²]
3000
2000
1000
0
b)
|𝓕 (v,w,Λ)|² [GeV⁻²]
200
100
0
c)
𝓕 (arbitrary units)
2.121
2.131
2.141
√v [GeV]

FIG. 2

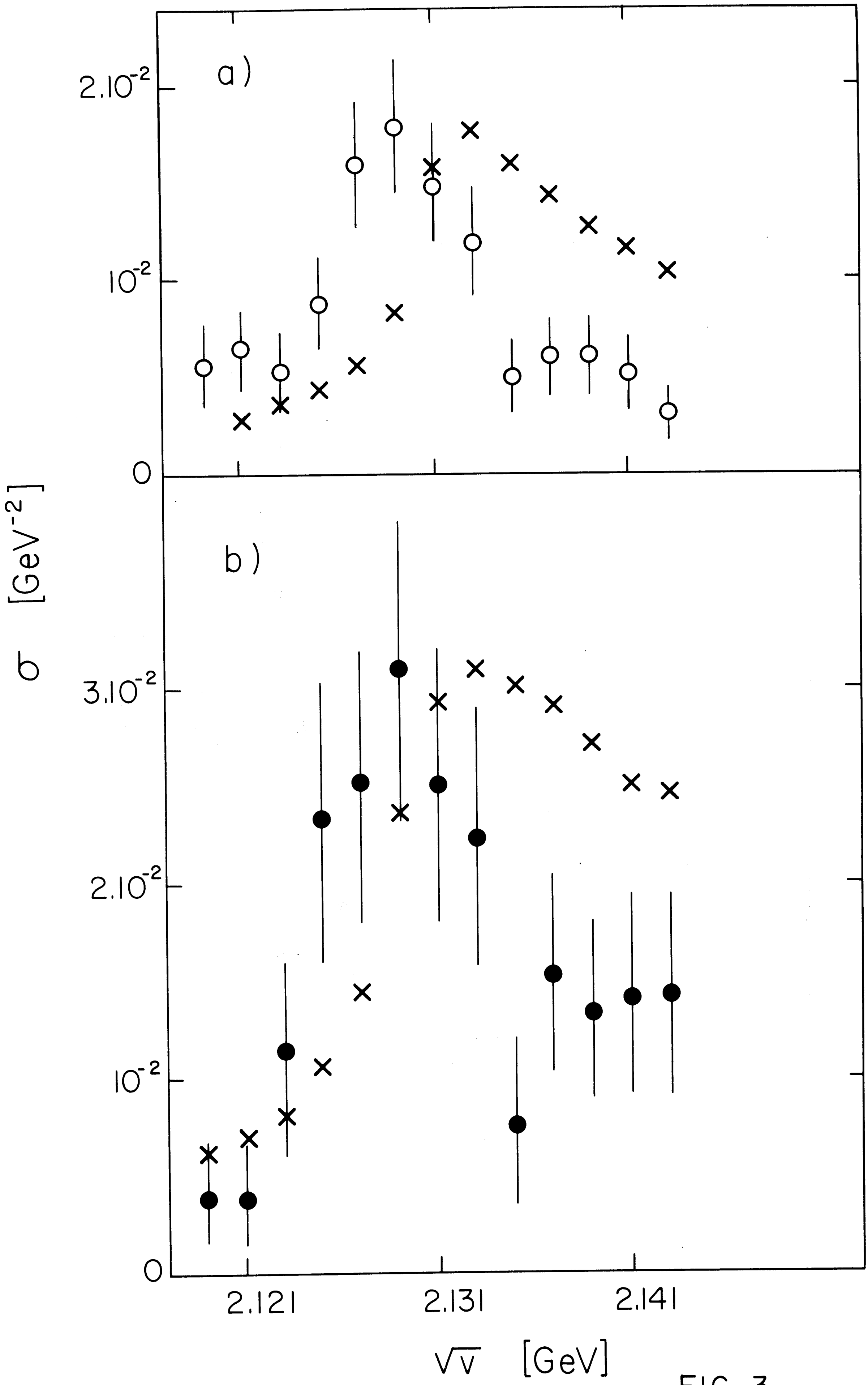

FIG. 3

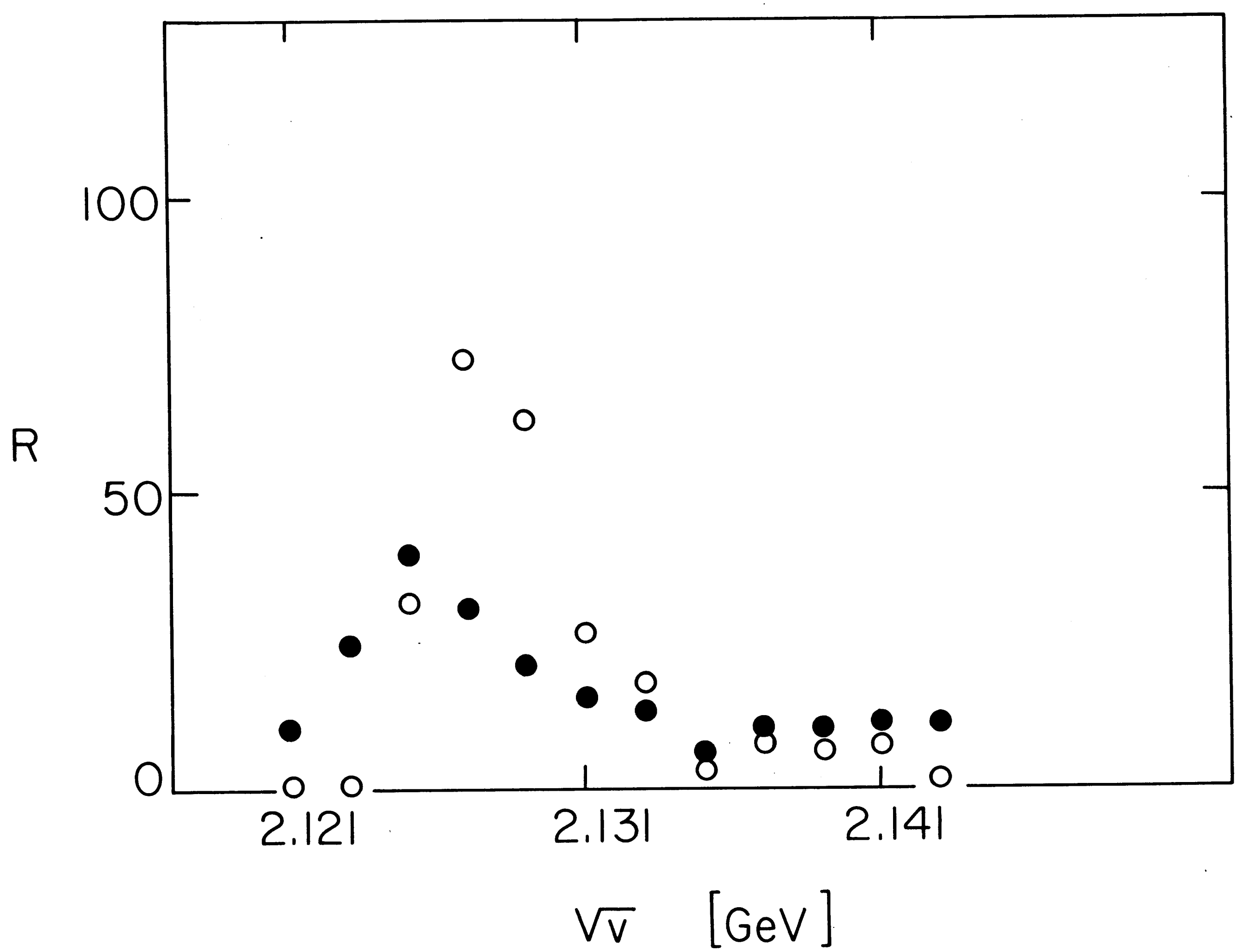

FIG. 4

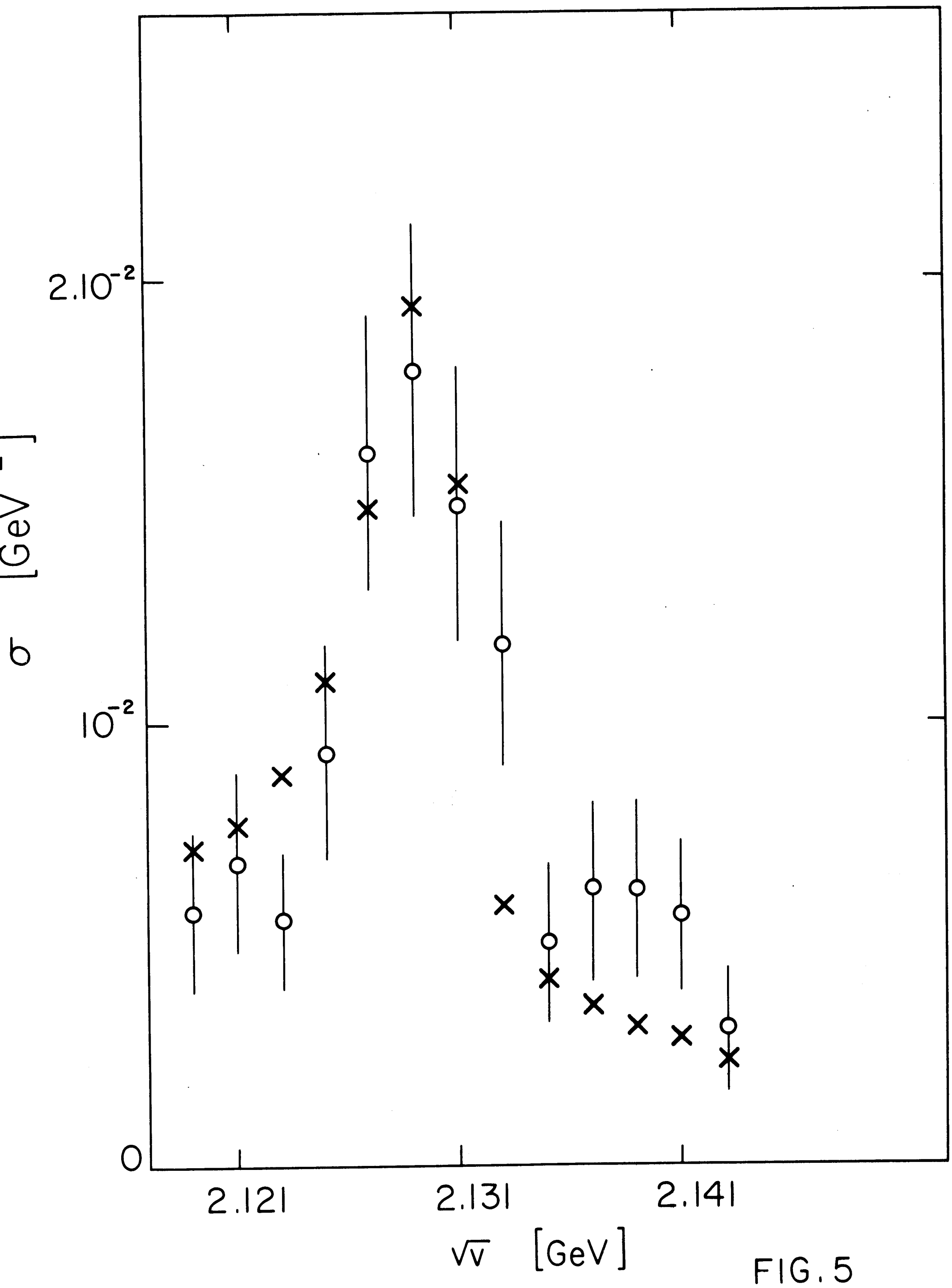

FIG. 5

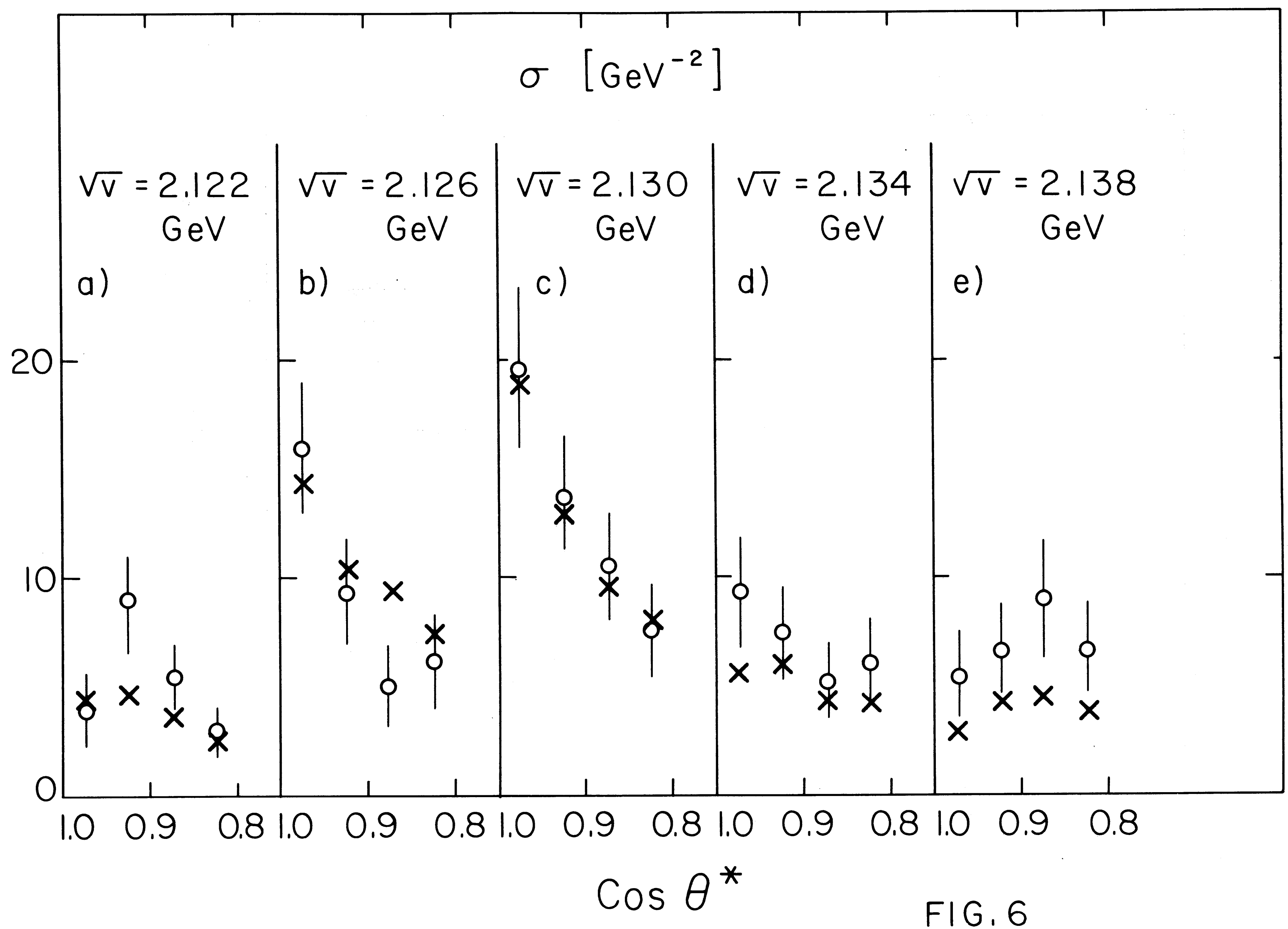
σ [GeV^-2]
√v = 2.122 GeV
a)
√v = 2.126 GeV
b)
√v = 2.130 GeV
c)
√v = 2.134 GeV
d)
√v = 2.138 GeV
e)
20
10
0
1.0
0.9
0.8
Cos θ*

FIG. 6